Electrochemical Detection of Dioctyl Phthalate using Molecularly Imprinted Polymer Modified Screen-printed Electrodes

HF EL Sharif[1], S Patel[1], EN Ndunda[2] and *SM Reddy[1]

[1]Department of Chemistry, School of Natural Sciences, University of Central Lancashire, Preston, PR1 2HE

[2]Department of Physical Sciences, Machakos University, P.O Box 136-90100, Machakos, Kenya

*corresponding author: smreddy@uclan.ac.uk

Abstract

We report the investigation of electropolymerised molecularly imprinted polymers (E-MIPs) for the determination of dioctyl phthalate (DOP). Low-cost and eco-friendly commercially available screen-printed electrodes (SPEs) were used. E-MIPs were produced using the cyclic voltammetry (CV) technique based on a water-soluble 4-aminophenol as functional monomer. E-MIPs for DOP showed affinity for the template, with 80% binding efficiency and an imprinting factor of 3. The E-MIPs were able to detect absolute levels of DOP in a time-dependent adsorption manner with the presence of 250 μg DOP (equivalent to 12.8 μM) detected in 5 minutes with a LOD (at 15 mins) of 177.1 μg and LOQ of 536.6 μg making them suitable for the measurement of DOP in freshwater when the sample is pre-concentrated.

Keywords

Molecularly imprinted polymers; MIPs; electrochemical polymerisation; biosensor; dioctyl phthalate (DOP); di(2-ethylhexyl) phthalate (DEHP); bis(2-ethylhexyl) phthalate; environmental monitoring; disposable electrodes.

Highlights

- Electropolymerisation of molecularly imprinted polymers (MIPs) on screen-printed electrodes (SPEs)
- Cu^{2+} coordination enhances MIP binding affinity
- Electrochemical detection of dioctyl phthalate (DOP) suitable for freshwater samples
- Real-time output for environmental monitoring

Graphical Abstract

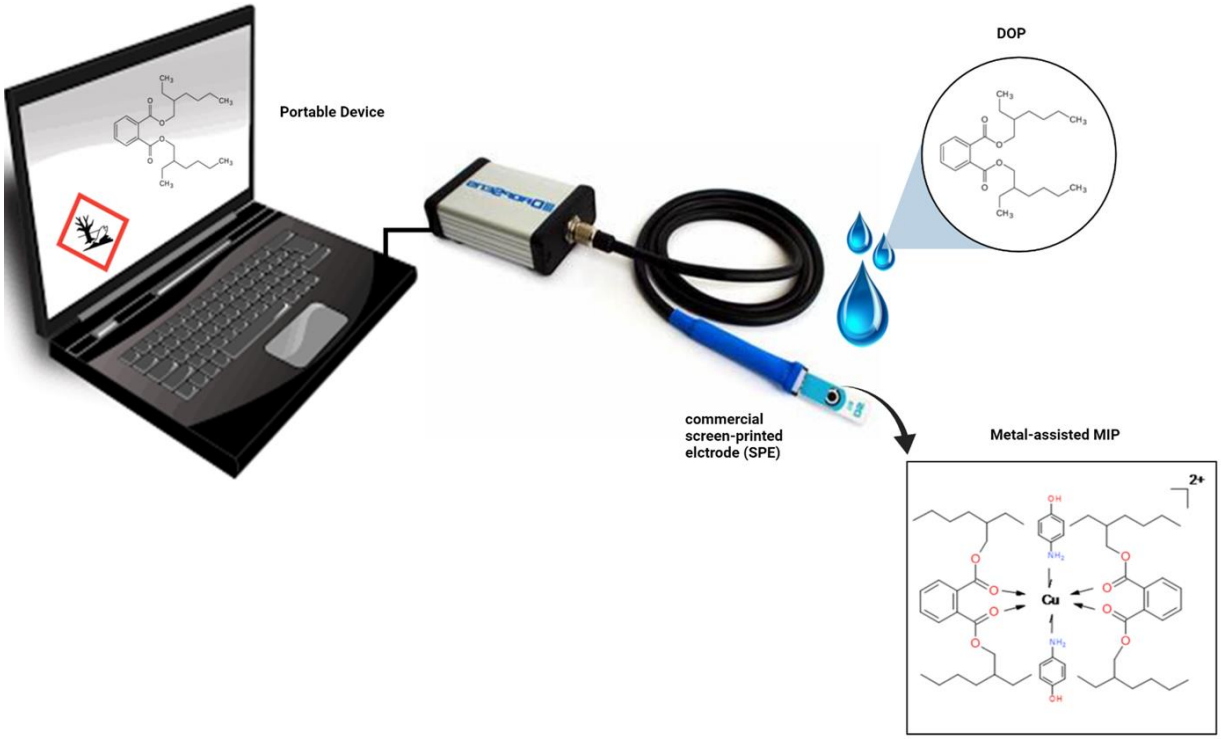

Introduction

Dioctyl phthalate (DOP) and its structural analogues are commonly used as plasticizers on an industrial scale to improve the flexibility and workability of polymeric materials. Through a variety of pathways such as industrial effluent and the presence of microplastics in waterways [1], they

invariably leak into the environment. Phthalate esters (PEs) are classified as xenoestrogens and endocrine disruptors, and their presence in the environment is a concern to human health and aquatic life. They can affect reproductive health and physical development [2]. They have been detected in Taiwan fish (2.4-253.9 mg/kg) [3] and in water in Kenya (0.07 - 27.20 µg/L) [4]. Their detection in the environment is mainly based on non-selective adsorbents for sample preparation and heavy GC-MS/ GC-FID investment albeit with a detection limit down to 1 µg/L.

Thus, there continues to be the need for affordable, portable, and selective techniques. While biological antibodies can also be used in diagnostic tests for environmental pollutants with precise results[5], antibodies are invariably unstable and require lengthy procedures to grow them in a host system or cell line and to isolate them before they can be used. Alternative to the use of antibodies, there is ongoing research in synthetic receptor technologies including aptamers [6] and molecularly imprinted polymers (MIPs) [7]. These offer the required guest-host type interactions with molecular targets which mimic antibody behaviour. MIPs offer the promise of a stable and cheap alternative to biological antibodies. They are easily produced in a one-step chemical reaction for the fraction of the price of antibodies. The target analyte serves as a template molecule around which a functional monomer self-assembles primarily through hydrogen bonding interactions. In the presence of an initiator and crosslinker, a polymer is grown effectively entrapping the target template. By and large, selectivity is conferred due to the cavity architecture that remains once the template molecule is removed. Selective rebinding is a function of the target template being recognised by the cavity. MIPs have been used extensively for small molecule (drug and pesticide) recognition. MIPs have also been used to recognise biomacromolecules including proteins [8, 9]. In the case of small molecule recognition, MIPs, in powder form have featured as solid phase extractants for target, isolating the compounds prior to introducing them to HPLC for determination [10, 11]. While chromatography offers a powerful lab-based separation tool, there is a need for multi-solvent reagents and regular maintenance to ensure the instrument works within acceptable parameters. MIPs in solid monolith format have been produced for selective phthalate extraction [12].

64 Recently, MIP selectivity for target has been enhanced with the inclusion of a metal ion capable of
65 complexing simultaneously with the target template and functional monomer prior to MIP
66 formation. Such metal assistance has been found to improve the spatial recognition of the template.
67 The metal centres such as Cu^{2+}, Co^{2+} or Zn^{2+} can form coordinate bonds between functional
68 monomer and target template [13-16], thus improving the binding affinity of the MIP binding sites
69 (cavities). In this work, Cu^{2+} was chosen based on its previous success within MIP integration for PEs
70 recognition. Its ability to coordinate with DOP by donor-acceptor interactions with two vacant sites
71 provides additional bond formation with NH_2 groups on the functional monomer [15].
72 Electrochemical analysis has become a mainstream analytical tool for the facile determination of
73 electrochemically active inorganic, organic and biologically active compounds [17-19]. However, not
74 all analytes (e.g. esters, antibodies, and DNA) are redox active at ambient electrode potentials
75 suitable for aqueous solution analysis (-1.0 to +1.0 V vs Ag/AgCl reference). They therefore do not
76 lend themselves to direct electrochemical interrogation. In such cases, alternative approaches have
77 been considered for their evaluation using the electrochemical method including the use of redox
78 markers such as potassium ferricyanide [20]. Recently, electropolymerisation has been exploited to
79 produce thin-film MIPs on electrode surfaces using redox active functional monomers such as
80 phenols, dopamine and o-phenylenediamine [21-23]. The target template is included in the
81 monomer solution and exposed to the working electrode. Cyclic voltammetry (CV) is used to induce
82 polymerisation of the functional monomer at the electrode surface to progressively grow the
83 polymer layer, requiring multiple sequential cycles for optimum film growth. The template, when
84 removed leaves binding sites selective for the rebinding of target. The subsequent rebinding of
85 target can be investigated also using CV. A small inorganic redox marker such as potassium
86 ferricyanide is used to probe the changing permeability of the MIP depending on whether the target
87 template is bound. In the bound state (when target is present), there is a reduced diffusion of redox
88 marker to the electrode and therefore a small current produced. In the eluted state (when target is
89 absent), the MIP is more permeable to the redox marker resulting in an increase in current. As

previously mentioned, esters are not electrochemically active in the potential window used for aqueous sample analysis. The ferro/ferricyanide redox system can be used as a ubiquitous redox marker for all electrode-based MIPs and obviates the need for the target itself to be electrochemically active. In an alternative electrochemical approach, semiconductor materials [[24]] and metal oxide frameworks [[25]] have been used to develop MIP-based photoelectrochemical (PEC) sensors for DOP. Due to the mechanism of photoelectron hole generation and subsequent reduction to generate a photocurrent, a suitable electron donor such as sodium sulphite is required. Whereas, in our system herein, the electrochemical current is dependent on the diffusion of ferrocyanide through the MIP, the photocurrent method is dependent on the diffusion of Na_2SO_3 through the MIP system. Whereas offering high sensitivity due to a large number of active sites, the semiconductor materials are prone to light corrosion due to rapid recombination of photogenerated electron hole pairs.

We investigate herein, the electrochemical growth and interrogation of a MIP for DOP, using 4-aminophenol (4-AP) as a functional monomer and ferro/ferricyanide as a redox probe. We present a combination of MIPs with copper ions to enhance the MIP-binding site and integration with commercially available disposable electrochemical chip technologies to develop new, simple, and disposable sensors for the measurement of DOP in water. MIPs are electrochemically grown and tethered to screen-printed electrode (SPE) surfaces which will elicit an array of electrochemical responses in the presence of phthalates. We will show that the selectivity of MIPs can be improved by introducing a metal centre during the MIP production process. The novelty of our approach is that we demonstrate the permanent integration of copper ions as part of the MIP/ electrochemical sensor composite. This has not been previously published to our knowledge. The sensitivity and stability of MIP-based sensors for PEs would make them attractive for rapid diagnostics as a simple screening tool.

Experimental Section

Materials

Dioctyl phthalate (DOP), copper chloride ($CuCl_2.2H_2O$), sulphuric acid (1 M), potassium ferricyanide, potassium chloride, phosphate buffer saline tablets (PBS, 10 mM, pH 7.4±0.2) and 4-aminophenol (4-AP) were purchased from Sigma-Aldrich (Poole, Dorset). All chemicals were of analytical grade and were used without further purification. PBS solutions were prepared using high-purity water from a Millipore Milli-Q system (resistivity ≥ 18 MΩ cm) and filter sterilised (0.2 µm filter). Disposable screen-printed electrodes (SPE) (Au-AT) comprising a gold working electrode (4 mm diameter), a gold counter electrode and silver reference electrode were purchased from Metrohm Dropsens (Runcorn, Cheshire).

Methods

Polymer layers using 50 µL depositions were fabricated directly onto Au-AT-SPE surfaces by electrochemical polymerisation using cyclic voltammetry (CV). Pre-polymer solutions were produced by dissolving 21 mg of 4-AP, 50 mg of $CuCl_2.2H_2O$ in 900 µL H_2SO_4 (0.5 M). DOP template was added in excess to give a final 10% (v/v) solution. To produce the MIP, the potential was cycled between 0.2 V and 1.2 V for 10 cycles at 50 mV s^{-1} (~ 8 min, room temperature (RT), 22±2 °C). To remove template DOP, elution was also carried out electrochemically (-0.5 V and 1.5 V for 5 cycles) at 175 mV s^{-1} (~ 5 min, RT, 22±2 °C) using PBS (50 µL) as electrolyte and elution medium. Non-imprinted polymers (NIP) were produced in the same manner but in the absence of DOP and taken through the elution process for consistency. To evaluate MIP selectivity and rebinding, the modified SPEs were exposed to 50 µL of DOP (0.5% w/v) solution in PBS (equivalent to 250 µg DOP) and CV and differential pulse voltammetry (DPV) data collected at 5 min intervals. All SPEs were characterised at each interval via typical CV/DPV scans (triplicate; 50 mV s^{-1}) using an externally loaded potassium ferricyanide solution (5 mM) containing 0.5 M KCl as supporting electrolyte (50 µL). All experiments were conducted using PSTrace5 software and a portable Emstat3 potentiostat (PalmSens) connected

to a PC laptop.

Results and Discussion

Electrochemical Characterization of E-MIP

E-MIP and corresponding E-NIP polymers were produced using cyclic voltammetry (CV) in PBS in the presence and absence of diluted DOP, respectively. Sulphuric acid (0.5 M) was required to solubilise the 4-AP functional monomer [26] in the electrosynthesis of the E-MIP-based DOP sensor. Copper chloride was also included in the polymerising solution to facilitate a coordination to occur between central copper ions, the functional monomer and DOP (Fig. 1). The copper was used as a spacer and mediator to optimise the so-called cavity or binding site within the MIP.

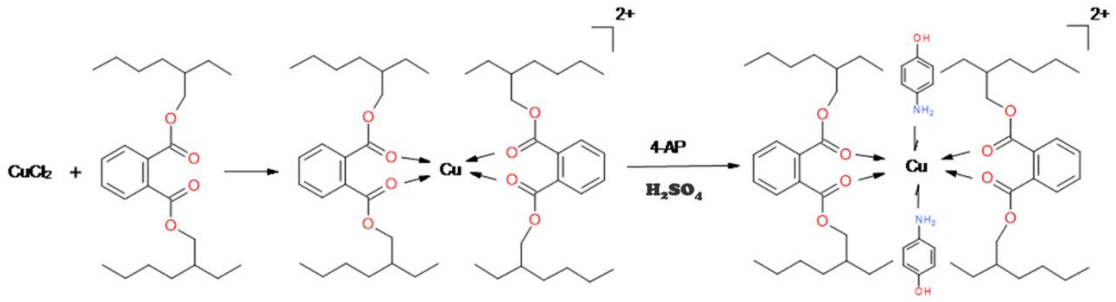

Fig. 1 - Proposed mechanism for copper-assisted self-assembly of template (DOP) with monomer (4-AP). Composed in Symyx draw 3.3.

Side redox reactions involving the Cu^{2+} being reduced to Cu^{+} or metallic copper which can occur at negative potentials [27] were avoided by keeping the scan range above +0.2 V (vs Ag/AgCl). Various scan speeds and cycle numbers were investigated to determine optimum conditions for DOP template capture during polymerisation (see supplementary; Fig. S1).

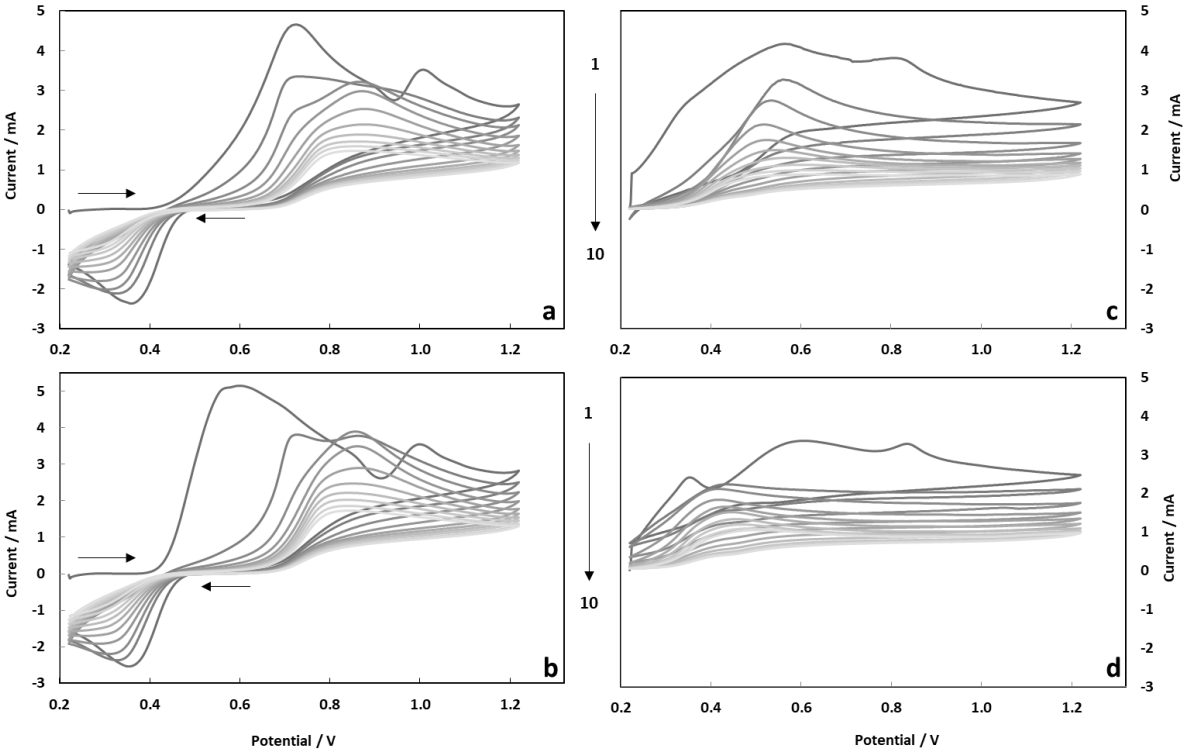

159

160 Fig.2 – CVs illustrating typical current responses in the 10 scan electropolymerisation process of 4-AP
161 in the presence of copper chloride for DOP MIP layers (a) and NIP layers (b); absence of copper
162 chloride DOP MIP layers (c) and NIP layers (d); all using H_2SO_4 (0.5 M) at a scan rate of 50 mV s^{-1}.

163

164 A total of ten cycles were found to be optimal to form stable and integral poly(4-AP) MIP and NIP
165 films adsorbed to the working electrode of the SPE (~ 8 min, RT, 22±2 °C). Fig. 2a and 2b show the
166 polymerisation cycles for E-MIP and E-NIP respectively. Two anodic peaks are observed initially (at
167 0.6 V and 0.97 V) attributed to formation of radical monocation ($4\text{-}AP^{\cdot+}$) and oxidation to dication
168 respectively. These peaks diminish with continuous cycling and are replaced by one broad anodic
169 peak mid-way between the two original peaks. On the negative sweep, only one of these anodic
170 peaks show complementary cathodic peaks at around 0.25 V. The progressive decrease in anodic
171 and cathodic peak currents with each cycle is an indicator that the 4-AP monomer is
172 electrochemically polymerising and adsorbing to the electrode surface. A proposed structural
173 mechanism for the synthesis of poly 4-AP is given in work by Thenmozhi et al. [28].

Fig. 2c and 2d also show the polymerisation cycles for E-MIP and E-NIP respectively in the absence of the metal mediator. It is interesting to note the anodic peaks due to 4-AP oxidation and polymerisation shift to higher potentials in the presence of copper, during and following the formation of E-MIP and E-NIP.

Following MIP or NIP formation, ferricyanide was used as a redox label to confirm that either E-MIP or E-NIP was deposited on the bare electrode. A diminution in peak current to the redox marker (compared with the bare electrode) was a firm indicator that a polymer layer was formed on the electrode surface. To remove (elute) DOP template, the voltage was cycled at more positive potentials (from -0.5 V up to 1.5 V) post-polymerisation in PBS (see supplementary; Fig. S2). This was found to effectively remove the template without apparently compromising the integrity of the pre-formed E-MIP.

Fig. 3 a and b compares the ferro/ferricyanide cyclic voltammograms on a bare electrode and following polymer formation, template elution and template rebinding for MIP and NIP respectively. The E-MIP follows the expected pattern in change in peak currents. There is a significant decrease in current upon MIP formation, compared with the bare electrode. Upon template elution, the anodic peak increases to an intermediate stage but still lower than the bare electrode, confirming that template has been removed (thus allowing more redox marker to diffuse to the electrode). Upon template rebinding, the peak current decreases due to a decrease in permeability of the redox marker to the electrode. The E-NIP also behaves as expected (Fig. 3b). The redox marker signal is much reduced following E-NIP formation, when compared with E-MIP formation. This points to a lower porosity and permeability within the NIP than the MIP, which is to be expected. The peak position shift (increase in potential) in oxidation and reduction peaks (and associated peak broadening) is expected. Prior to DOP addition, the polyphenol-based MIP layer contains DOP-selective cavities (pores) which allows relatively unimpeded access of ferricyanide to the SPE electrode surface. However, upon the addition of increasing concentration of DOP (an insulating and

non-conducting material), this selectively binds within the MIP cavities, blocking the path for ferricyanide transport to the electrode and subsequently introduces an increasingly insulating barrier to diffusion of the redox marker to the electrode surface resulting in the observed decrease in ferri/ferrocyanide peak current and an associated shift (increase) in peak position to more positive potentials.

The absence of template in the E-NIP production confers that film formation progresses unimpeded during the polymerisation cycles allowing the production of a dense polymer layer. The NIP layer is expected to be more uniform and homogenously produced compared with the MIP. The presence of the template, DOP, serves to impede the otherwise natural course of monomer polymerisation and crosslinker incorporation. The polymerisation process therefore needs to navigate around the template and entraps it between the growing polymer chains during the process resulting in a more porous polymer layer structure on the electrode. Polymer growth in the NIP, by contrast, is less tortuous allowing it to form a more rigidly coupled, homogeneous and dense layer with inherently low porosity.

Therefore, for an equivalent number of polymerisation cycles, the NIP will incorporate more monomer than the MIP. With the assistance of the Cu^{2+} ions, an initial pre-polymerisation complex can be formed between DOP, copper and the 4-AP monomer. This pre-polymer complex (as proposed in Fig. 1) appears to be crucial in improving cavity affinity for DOP rebinding. Further, since there is no template to remove in the NIP, subsequent elution cycling also confirms that electrochemical elution conditions do not affect the integrity of the polymer layer.

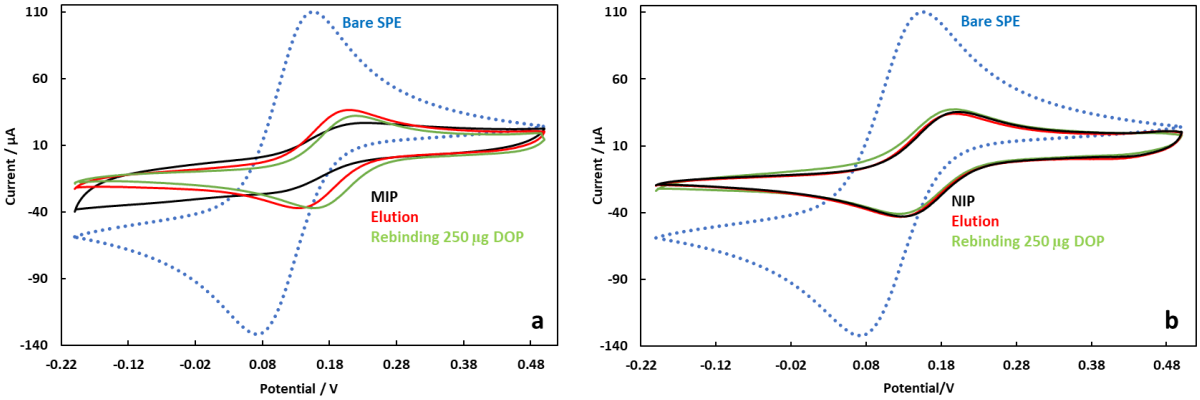

219

220 Fig.3 – CV characterisations using a 5 mM potassium ferricyanide solution containing 0.5 M KCl as
221 supporting electrolyte (50 µL, triplicate, 50 mV s^{-1}) illustrating the current responses for SPEs
222 modified with MIP before elution; MIP after elution; MIP after rebinding 250 µg DOP in PBS solution
223 (a) and NIP before elution; NIP after elution; NIP after rebinding DOP (b).

224

225 Fig. 4 compares DOP (250 µg DOP in 50 µL PBS solution; equivalent to 5 mg/mL or 12.8 µM)
226 rebinding to MIP with and without metal ion assistance during polymerisation. In these rebinding
227 studies, copper assistance radically improves the rebinding efficiency and selectivity for the
228 template. Whereas, there is no significant change in the redox marker signal with metal-unassisted
229 MIP (MU-MIP), there is a clear and measurable decrease in anodic peak of the redox marker
230 following DOP rebinding on MIP with metal assistance (MA-MIP) due to copper pre-treatment.
231 Additionally, our results suggest that once the complex is consolidated during MA-MIP formation,
232 the copper persists within the polymer even during the elution cycles and produces a more compact
233 polymer layer.

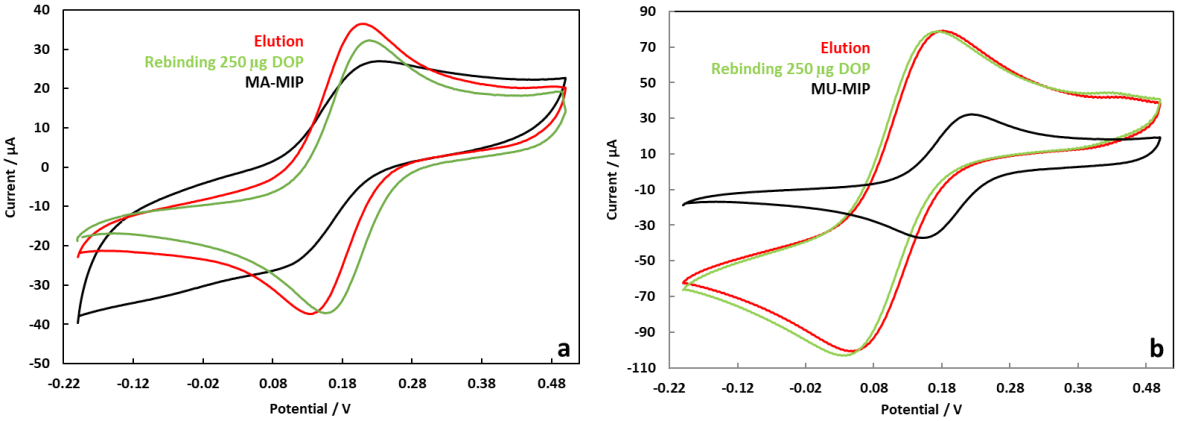

234

235 Fig. 4 - CV characterisations using a 5 mM potassium ferricyanide solution containing 0.5 M KCl as
236 supporting electrolyte (50 µL, triplicate, 50 mV s^{-1}) illustrating DOP (250 µg DOP in PBS solution; i.e.
237 0.5% w/v)) rebinding to MIP with (a) and without (b) metal ion assistance during polymerisation.

238

239 Confirmation was sought using SEM-EDX of MA-MIP before and after template elution to
240 demonstrate the presence of polymer modification and topography change (Fig. 5); while also
241 demonstrating the residual presence of metal ions within the polymer. Characteristic copper peaks
242 (2000 counts at 1 keV) could be observed in freshly prepared MA-MIP, and the peaks remained upon
243 subsequent elution (see supplementary; Fig. S3). There appears to be a hysteresis effect in the MA-
244 MIP where copper inclusion has aided and improved the polymer cavity architecture leading to
245 improved rebinding of DOP to MIP. This is in line with other recent reports where metal ion inclusion
246 during both imprinting and rebinding stages has improved MIP affinity for template [15], but our
247 findings appear to be the first report of the metal playing a semi-permanent role in improving the
248 binding site characteristics during both the MIP formation and rebinding processes.

249

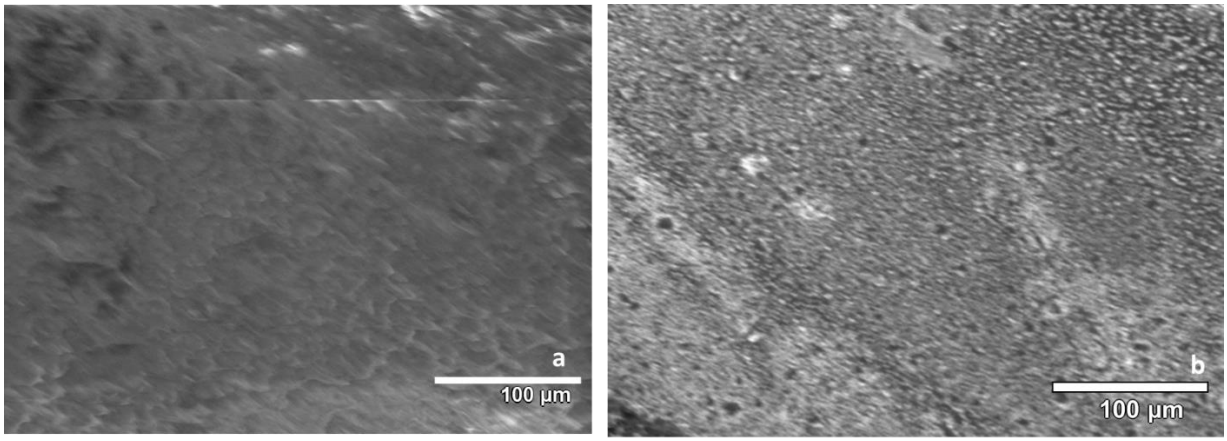

Fig.5 - SEM-EDX scans of MA-MIP before (a) and after (b) elution demonstrating the presence of polymer modification and topography change. Scans were conducted using a JCM-6000PLUS at the set parameters of 15.0 kV, Probe Current: 7.47500 nA. SPEs were measured in triplicate using 3 different sites.

DOP Detection using E-MIPs

Fig. 6a shows the effect on the ferricyanide differential pulse voltammetry (DPV) signal with time (5-minute intervals) upon reloading DOP into MIP over a 25-minute period in PBS buffer solution. The signal decreases as expected with time as the DOP binding sites become occupied, thereby preventing diffusion of redox marker to the electrode; and reaching a saturation point at 20 minutes. When absolute values of the change in peak current are plotted against time over a 30-minute period (Fig. 6b), we can directly compare the effect of DOP binding to MIP and NIP. With MIP, as stated, there is an initial linear increase in current change with exposure time reaching a saturation (plateau) at 15-20 min. With the NIP, there is, as expected, a lower level of DOP binding (due to non-specific binding) and a linear relationship between current change and DOP exposure time. The MIP:NIP current change ratios (equated to relative imprinting factors) at 5 min and 10 min DOP exposure are 3.1 and 3 respectively. Therefore, we propose absolute levels of 250 µg of DOP in can be detected reliably within 5 min using our method.

Given that the MIPs were able to detect the presence of DOP in less than 10 minutes, then by extrapolation a limit of detection (LOD) of 177.09±95.83 μg (equivalent to 3.5 mg/mL; 9 μM)) and a limit of quantification (LOQ) of 536.64±119.59 μg DOP were determined for our E-MIP based on poly(4-aminophenol) insulating polymer. LOD and LOQ were calculated based on the linear dynamic range (LDR) at 3.3σ and 10σ respectively. Using a similar electrochemical approach but with a polypyrrole conducting polymer as the E-MIP material, Bolat et al. [29] reported a detection range between 0.01–1.0 μM of dibutylphthalate. Our DOP-MIP screen-printed electrode device is suitable for the measurement of DOP in PBS, but some sample concentration would be required. As required with chromatographic techniques [30], for both our E-MIP system and that of Bolat et al., the water sample would need to be first pre-concentrated using, for example, solid phase extraction [31] allowing for pre-concentration factors of 600 to 1000 in order to be able to measure down to the WHO recommended levels of 5 μg/L (12.8 nM) of DOP. We performed experiments using DOP (2.5 mg/mL) spiked in tap water. The sample was diluted in PBS prior to electrochemical analysis. We demonstrate that we can determine the presence of DOP, with 98.5% recovery following 25 min of exposure of sample to the sensor.

Recently a MIP layer based on o-phenylenediamine, selective for DOP, was electrochemically grown on the bismuth sulphide (Bi_2S_3) layer [24]. In the latter study, EIS was used to interrogate the MIP and corresponding NIP. Bespoke ITO electrodes were modified with Bi_2S_3, a metal chalcogenide semiconductor. The photoelectrochemical sensor apparently demonstrated pM sensitivity to DOP and selectivity when tested against other phthalate esters. The Bi_2S_3 layer has photoelectric properties which can be interrogated electrochemically, but it was not very clear from the paper what the mechanism was that allowed Bi_2S_3 to be a superior sensitive material to electrochemically detect DOP in the MIP overlayer. Also, given the multi-step approach requiring Bi_2S_3 synthesis, its attachment to ITO followed by electrochemical growth of MIP layers, the reproducibility of each step is not discussed.

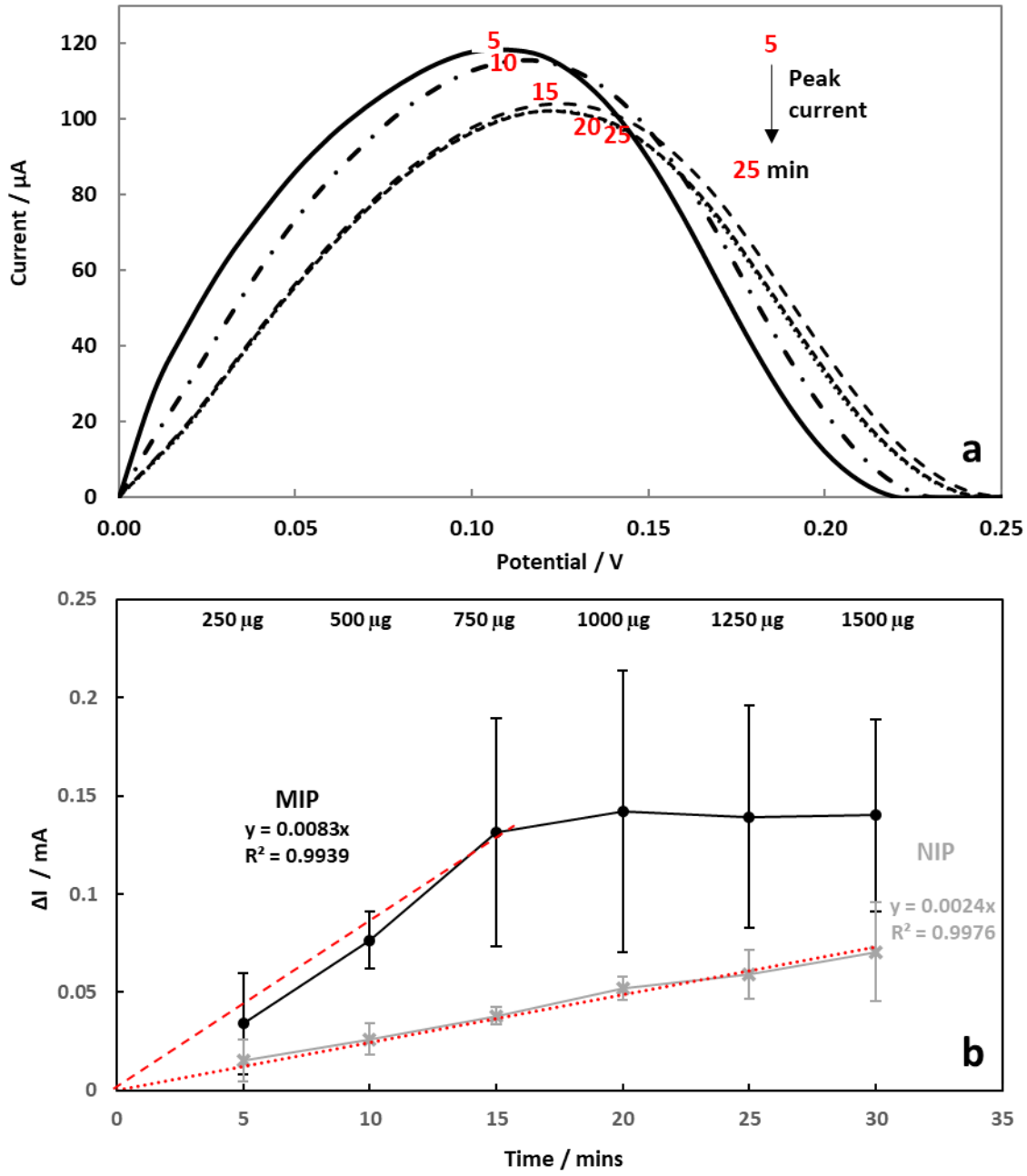

294

295 Fig.6 – (a) DPV characterisation of diminishing ferricyanide signal with DOP rebinding to MIP taken at
296 5, 10, 15, 20 and 25 minutes (note DPV curves at 20 and 25 min are superimposed); (b) Kinetics of
297 rebinding 50 µL of DOP (250 µg) onto MIP (▪) and NIP (X) in PBS. LOD and LOQ were calculated based
298 on the LDR at 3.3σ and 10σ respectively. Data represents mean ± SD, n=3.

299

The feasibility of re-using our E-MIP modified SPEs for DOP detection was also investigated. Fig. 7 demonstrates that the DOP-MIP is suitable for single use only. After a first rebind (where DPV peak moves from curve 1 to 2) and subsequent DOP elution (where DPV peak moves from curve 2 to 3), attempts at a second (or third rebind) results in a ferro/ferricyanide oxidation peak returning to that of the bare electrode (i.e. DPV peaks move from curve 3 to 4), suggesting that the MIP layer has been removed. Therefore, the device is not feasible for multiple uses or real-time monitoring but is reliable for single use.

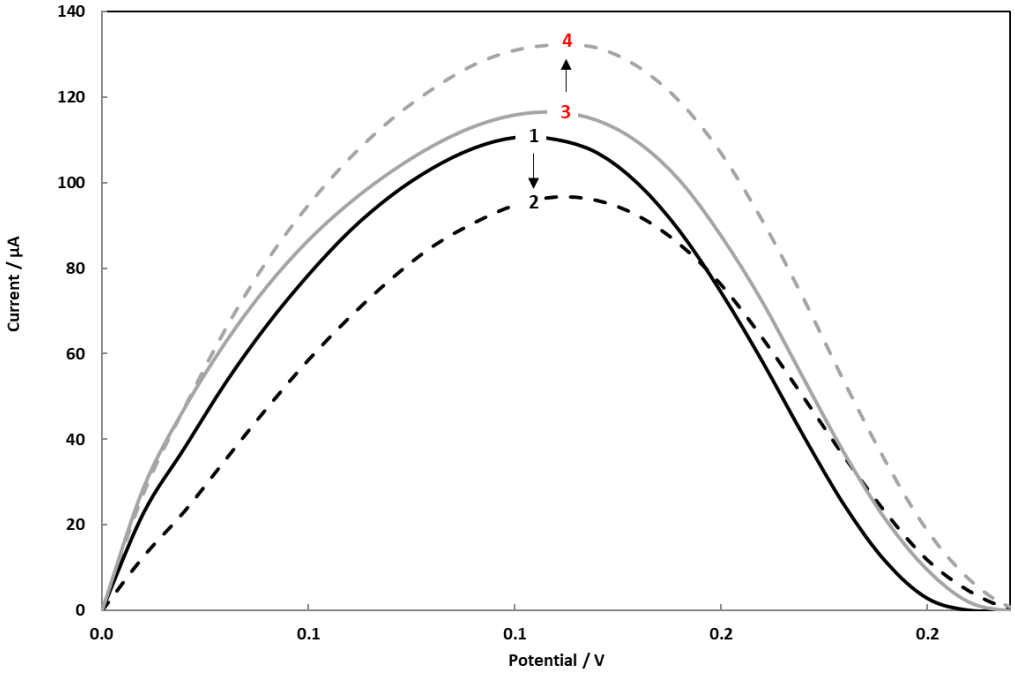

Fig.7 – DPV characterisation of ferricyanide signals with 250 µg DOP rebinding to MIP taken after 5 min using a first elution (curve 1 to curve 2) and post a second elution (curve 3 to curve 4).

Conclusions

We have shown that 4-aminophenol can be used a functional monomer for the imprinting and determination of DOP. MIP affinity is improved with Cu^{2+} ion assistance facilitating a coordination between monomer, metal ion and DOP to form the selective cavity is proposed. We have demonstrated that the metal ion persists within the polymer post-elution of the template and is

crucial to improving the binding affinity of DOP to MIP but not NIP, suggesting that the metal is indeed assisting template selective rebinding within a so-called cavity of the MIP. We offer a simple electrochemical method to prepare DOP sensitive MIPs. Further work is required to better understand the selectivity and compatibility of the MIPs within real samples.

Author Contributions

SP, HELS, and SMR contributed to conception and design of the study. SP and HELS performed the study and analysis. SMR, HELS and SP wrote the manuscript. All authors contributed to manuscript revision, read and approved the submitted version.

Conflict of Interest Statement

The authors declare that the research was conducted in the absence of any commercial or financial relationships that could be construed as a potential conflict of interest.

Acknowledgments

The authors wish to thank UCLan internship funding and The Royal Society (IES/R3/190093) for supporting this work. The authors also gratefully acknowledge the assistance of Peter Bentley for conducting SEM.

References

1. Segovia-Mendoza, M., et al., *How microplastic components influence the immune system and impact on children health: Focus on cancer.* Birth Defects Research, 2020. **112**(17): p. 1341-1361.
2. Mima, M., D. Greenwald, and S. Ohlander, *Environmental Toxins and Male Fertility.* Current Urology Reports, 2018. **19**(7).
3. Lee, C.-C., et al., *Emergent contaminants in sediments and fishes from the Tamsui River (Taiwan): Their spatial-temporal distribution and risk to aquatic ecosystems and human health.* Environmental Pollution, 2020. **258**.
4. Chepchirchir, B.S., A. Paschke, and G. Schueuermann, *Passive sampling for spatial and temporal monitoring of organic pollutants in surface water of a rural-urban river in Kenya.* Science of the Total Environment, 2017. **601**: p. 453-460.

5. Li, L. and M.C. Zhang, *Development of immunoassays for the determination of phthalates.* Food and Agricultural Immunology, 2020. **31**(1): p. 303-316.
6. Warsinke, A. and B. Nagel, *Towards separation-free electrochemical affinity sensors by using antibodies, aptamers, and molecularly imprinted polymers - A review.* Analytical Letters, 2006. **39**(13): p. 2507-2556.
7. Shi, R.X., et al., *The development of research in molecular imprinting technique.* Progress in Chemistry, 2002. **14**(3): p. 182-191.
8. Yang, K., et al., *Protein-imprinted materials: rational design, application and challenges.* Analytical and Bioanalytical Chemistry, 2012. **403**(8): p. 2173-2183.
9. Culver, H.R. and N.A. Peppas, *Protein-Imprinted Polymers: The Shape of Things to Come?* Chemistry of Materials, 2017. **29**(14): p. 5753-5761.
10. Fernandez-Ramos, C., et al., *Analysis of trace organic compounds in environmental, food and biological matrices using large-volume sample injection in column-switching liquid chromatography.* Trac-Trends in Analytical Chemistry, 2014. **62**: p. 69-85.
11. Kanu, A.B., *Recent developments in sample preparation techniques combined with high-performance liquid chromatography: A critical review.* Journal of Chromatography A, 2021. **1654**.
12. Yusof, N.F., F.S. Mehamod, and F.B.M. Suah, *Adsorptive removal of bis(2-ethylhexyl) phthalate using an imprinted polymer: isotherm and kinetic modelling.* International Journal of Environmental Analytical Chemistry, 2020.
13. Striegler, S., *Designing selective sites in templated polymers utilizing coordinative bonds.* Journal of Chromatography B-Analytical Technologies in the Biomedical and Life Sciences, 2004. **804**(1): p. 183-195.
14. Recillas Mota, J.J., et al., *Synthesis and characterization of molecularly imprinted polymers with metallic zinc center for enrofloxacin recognition.* Reactive & Functional Polymers, 2013. **73**(8): p. 1078-1085.
15. Kaur, P., et al., *Metal Assisted Approach to Develop Molecularly Imprinted Mesoporous Material Exhibiting Pockets for the Fast Uptake of Diethyl Phthalate as Copper Complex.* Analytical Sciences, 2014. **30**(5): p. 601-607.
16. El-Sharif, H.F., et al., *Highly selective BSA imprinted polyacrylamide hydrogels facilitated by a metal-coding MIP approach.* Acta Biomaterialia, 2015. **28**: p. 121-127.
17. Liu, Z.-G. and X.-J. Huang, *Voltammetric determination of inorganic arsenic.* Trac-Trends in Analytical Chemistry, 2014. **60**: p. 25-35.
18. Khanmohammadi, A., et al., *An overview to electrochemical biosensors and sensors for the detection of environmental contaminants.* Journal of the Iranian Chemical Society, 2020. **17**(10): p. 2429-2447.
19. Wu, Q., H.-M. Bi, and X.-J. Han, *Research Progress of Electrochemical Detection of Heavy Metal Ions.* Chinese Journal of Analytical Chemistry, 2021. **49**(3): p. 330-340.
20. Lee, S., W.J. Kim, and M. Chung, *Enhanced electrochemical biosensing on gold electrodes with a ferri/ferrocyanide redox couple.* Analyst, 2021.
21. Yarman, A. and F.W. Scheller, *The First Electrochemical MIP Sensor for Tamoxifen.* Sensors, 2014. **14**(5): p. 7647-7654.
22. Ribeiro, J.A., et al., *Electrochemical detection of cardiac biomarker myoglobin using polyphenol as imprinted polymer receptor.* Analytica Chimica Acta, 2017. **981**: p. 41-52.
23. Liu, Y.Y., et al., *A highly sensitive and selective electrochemical sensor based on polydopamine functionalized graphene and molecularly imprinted polymer for the 2,4-dichlorophenol recognition and detection.* Talanta, 2019. **195**: p. 691-698.
24. Li, X.Q., et al., *A molecularly imprinted photoelectrochemical sensor based on the use of Bi2S3 for sensitive determination of dioctyl phthalate.* Microchimica Acta, 2019. **186**(11).

25. Gao, P.W., et al., *High-sensitivity photo-electrochemical heterostructure of the cuprous oxide-metal organic framework for a dioctyl phthalate molecularly imprinted sensor.* Analyst, 2021. **146**(20): p. 6178-6186.
26. Ferreira, L.F., et al., *Gold electrodes modified with poly (4-aminophenol): incorporation of nitrogenated bases and an oligonucleotide.* Polymer International, 2008. **57**(4): p. 644-650.
27. Gomaa, E.A., R.R. Zaky, and M.S. Nouh, *Cyclic Voltammetry Studies for the Interaction of $CuCl_2$ with 4-Fluoro Benzoic Acid (FBA) in KBr Aqueous Solutions.* Advanced Journal of Chemistry-Section A, , 2020. **3**: p. S583–S593.
28. Thenmozhi, G., P. Arockiasamy, and R. Jaya Santhi, *Isomers of Poly Aminophenol: Chemical Synthesis, Characterization, and Its Corrosion Protection Aspect on Mild Steel in 1M HCl.* International Journal of Electrochemistry, 2014. **2014(3)**: p. 1-11.
29. Bolat, G., Y.T. Yaman, and S. Abaci, *Molecularly imprinted electrochemical impedance sensor for sensitive dibutyl phthalate (DBP) determination.* Sensors and Actuators B-Chemical, 2019. **299**.
30. Lv, X.J., Y. Hao, and Q. Jia, *Preconcentration Procedures for Phthalate Esters Combined with Chromatographic Analysis.* Journal of Chromatographic Science, 2013. **51**(7): p. 632-644.
31. Li, J.D., et al., *Analysis of phthalates via HPLC-UV in environmental water samples after concentration by solid-phase extraction using ionic liquid mixed hemimicelles.* Talanta, 2008. **74**(4): p. 498-504.

Supplementary Figures

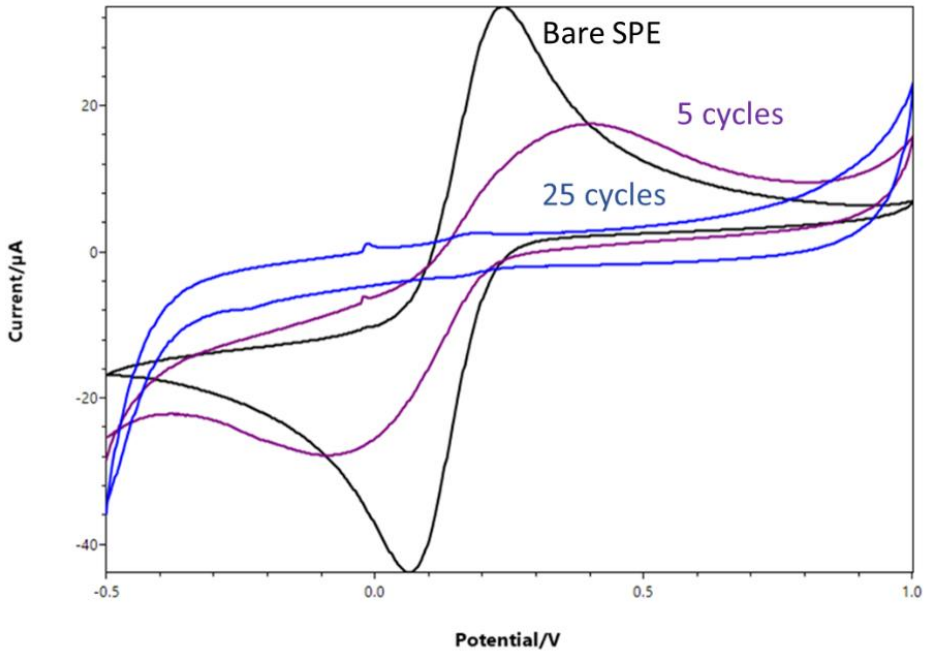

Fig. S1 – CV characterisations using a 5 mM potassium ferricyanide solution containing 0.5 M KCl as supporting electrolyte (50 µL, triplicate, 50 mV s^{-1}) illustrating the current responses for SPEs modified at various cycle number of electropolymerisation process of 4-AP in the presence of copper chloride for DOP MIP layers, scan rate of 50 mV s^{-1}.

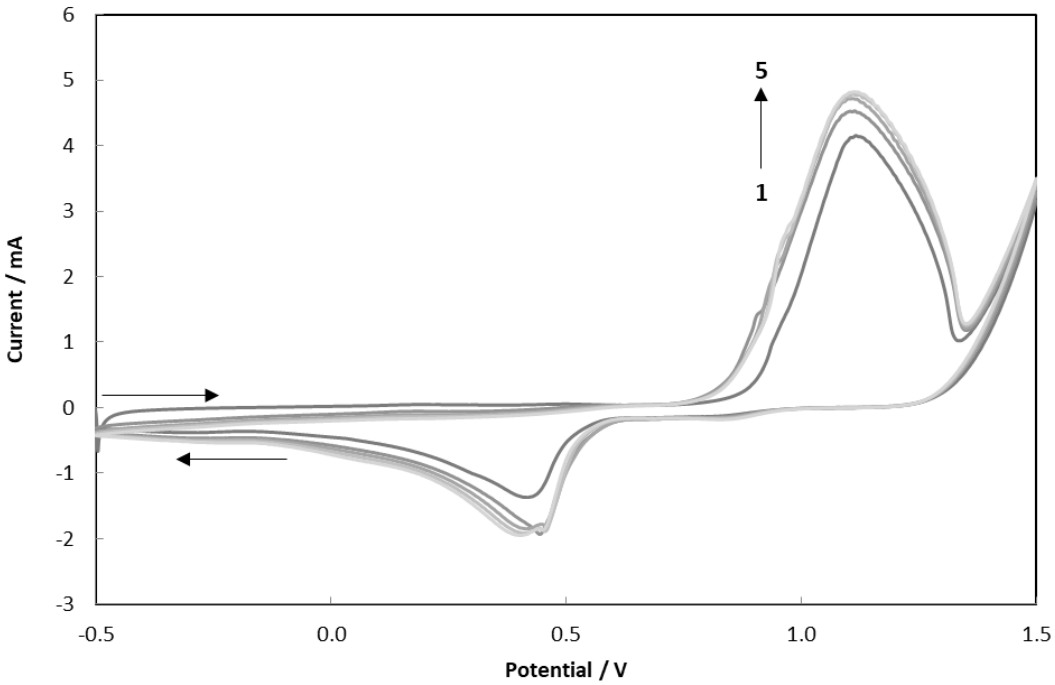

419

420 Fig. S2 - CV illustrating a typical DOP template elution process with 5 cycles at 175 mV s^{-1} (~ 5 min,

421 RT, 22±2 °C) using PBS (50 µL).

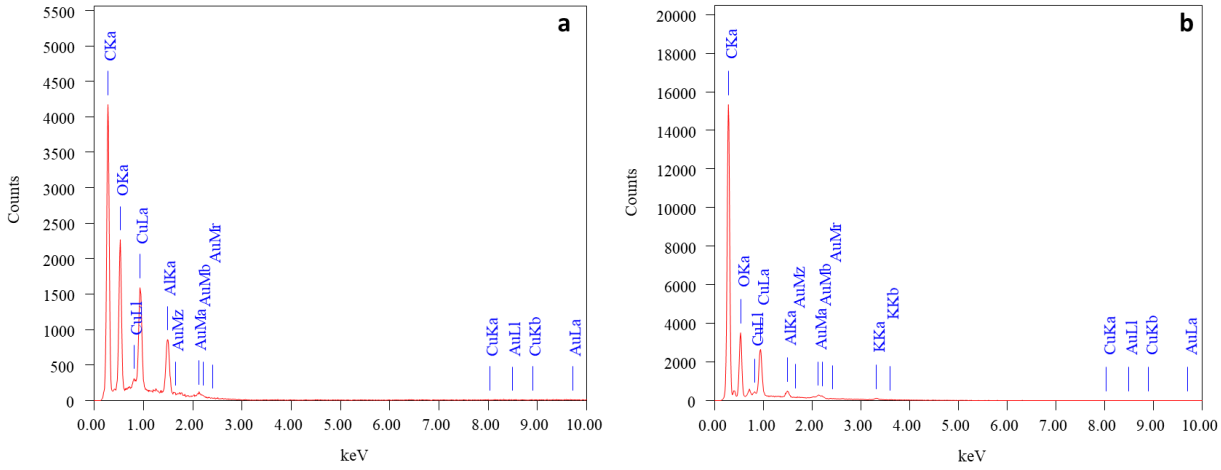

422

423 Fig. S3 - SEM-EDX scans of MA-MIP before (a) and after (b) elution demonstrating the residual

424 presence of metal ions within the polymer. Scans were conducted using a JCM-6000PLUS at the set

425 parameters of 15.0 kV, Probe Current: 7.47500 nA, ZAF Method Standardless quantitative analysis,

426 fitting coefficient: 0.0762. SPEs were analysed in triplicate using 3 different sites.